ISSN 0026-8933, Molecular Biology, 2022, Vol. 56, No. 3, pp. 453–462. © The Author(s), 2022. This article is an open access publication.
ISSN 0026-8933, Molecular Biology, 2022. © The Author(s), 2022. This article is an open access publication.

MOLECULAR CELL BIOLOGY

Multimodal Magnetic Resonance and Fluorescence Imaging of the Induced Pluripotent Stem Cell Transplantation in the Brain

Y. C. Zhang[a, b], J. W. Wang[b, c], Y. Wu[b, c], Q. Tao[d], F. F. Wang[b, c], N. Wang[a, b], X. R. Ji[a, b], Y. G. Li[d], S. Yu[a, b, *], and J. Z. Zhang[a, b, c, e, **]

[a] *University of Science and Technology of China, Hefei, 230026 P.R. China*

[b] *Suzhou Institute of Biomedical Engineering and Technology, Chinese Academy of Sciences, Suzhou, 215163 P.R. China*

[c] *Zhengzhou Institute of Engineering and Technology Affiliated with SIBET, Zhengzhou, 450001 P.R. China*

[d] *Department of Radiology, The First Affiliated Hospital of Soochow University, Suzhou, 215100 P.R. China*

[e] *Tianjin Guokeyigong Science and Technology Development Company Limited, Tianjin, 300399 P.R. China*

**e-mail: yush@sibet.ac.cn*

***e-mail: zhangjz@sibet.ac.cn*

Received September 27, 2021; revised November 11, 2021; accepted November 25, 2021

Abstract—The understanding of the engrafted cell behaviors such as the survival, growth and distribution is the prerequisite to optimize cell therapy, and a multimodal imaging at both anatomical and molecular levels is designed to achieve this goal. We constructed a lentiviral vector carrying genes of ferritin heavy chain 1 (*FTH1*), near-infrared fluorescent protein (*iRFP*) and enhanced green fluorescent protein (*egfp*), and established the induced pluripotent stem cells (iPSCs) culture stably expressing these three reporter genes. These iPSCs showed green and near-infrared fluorescence as well as the iron uptake capacity in vitro. After transplanted the labeled iPSCs into the rat brain, the engrafted cells could be in vivo imaged using magnetic resonance imaging (MRI) and near-infrared fluorescent imaging (NIF) up to 60 days at the anatomical level. Moreover, these cells could be detected using EGFP immunostaining and Prussian blue stain at the cellular level. The developed approach provides a novel tool to study behaviors of the transplanted cells in a multimodal way, which will be valuable for the effectiveness and safety evaluation of cell therapy.

Keywords: multimodal imaging, magnetic resonance imaging, fluorescent imaging, cell therapy, brain

DOI: 10.1134/S0026893322030153

INTRODUCTION

Cell therapy, promoting the regeneration of dysfunctional or injured tissue by transferring the intact stem cells or their derivatives to the targeted organs, has offered great promise for new medical treatments [1]. Giving the fact that engrafted living cells have the capacity of self-renewal and multi-differentiation, it is of importance to understand the in vivo behaviors of these cells including the survival, growth, distribution and integration.

The transplanted cells have to be efficiently labeled for better visualization and tracking in vivo. So far, the labeling strategies have been divided into two categories: direct imaging by using contrast agents such as dyes, radioactive tracers or magnetic particles, or the reporter-based method by labeling the target cells with exogenous reporter genes. The direct labeling is easy to manipulate, but the proliferation of labeled cells and phagocytosis by macrophages will make the signal fade over time. Moreover, a signal from the living and dead cells could not be distinguished by this method [2–4]. In contrast, the reporter-based strategy is more reliable and specific for tracing the transplanted cells, since the reporter genes will be introduced into the cellular genomic DNA and transferred equally to the daughter cells [5–7]. The detailed comparison of these two labeling strategies was summarized in Table 1.

Various imaging methods to track the engrafted cells have developed, and each imaging technique has its imaging range, advantages as well as limitations [4, 8]. For example, magnetic resonance imaging (MRI) provides excellent soft-tissue contrast and functional, structural and morphological information, however, it could not provide information at the molecular or cellular level [9]. Optical imaging like green fluorescent protein (GFP) could be imaged at a single cell level, however, the limited penetration depth impedes its application in deep tissue imaging. The advantages and limitations of the most used imaging techniques are summarized in Table 2 [4, 7, 8]. It is clear that no single-mode imaging modality combines all the advantages and better than the other techniques. Therefore, a multimodal imaging method, which visualize the anatomical and cellular events at different

Table 1. Comparison of the direct and reporter-based labeling strategies

Imaging strategy	Labeling method	Advantages	Disadvantages
Direct imaging	Fluorescent dyes, radioactive substances, magnetic particles such as SPIO	(1) Easy to manipulate (2) Bring no genetic modification to the labeled cells	(1) Signal diluted by cell proliferation and phagocytosis (2) Both viable and dead cells produce signals (3) Phagocytosis leads to unspecific labeling of the target cells (4) Toxicity of contrast agents
Reporter-based imaging	Introducing exogenous reporter genes by genetic manipulation	(1) Specifically label the target cell types (2) Only viable cells can be traced in vivo (3) Signals do not fade due to cell proliferation	(1) Introduce genetic modification to the labeled cells (2) Rather complex manipulation

levels via deploying multiple reporter genes detectable by different imaging modality is at present a hotspot of the imaging research.

In the recent years, the combination of PET/MRI, bioluminescence imaging (BLI)/MRI, PET/BLI have been successfully developed and introduced into the clinical application [4]. However, the combination of imaging techniques at both microscale and macroscale levels is still in progress. In the present study, we prepared a lentivirus carrying multimodal reporters FTH1, iRFP and EGFP and established the induced pluripotent stem cell (iPSCs) culture stably expressing these labeled genes. We showed that the combination of the three reporters ensured the long-term detection of these transplanted cells by MRI and near-infrared fluorescent (NIF) imaging at the anatomical level, as well as by immunostaining and Prussian blue stain at the cellular level. Our study provides a novel tool to study the cellular behaviors of the transplanted cells in a multimodal way, which will be valuable for the effectiveness and safety evaluation of cell therapy.

EXPERIMENTAL

iPSCs culture. iPSCs (kindly provided by Guangzhou Stem cell and Regenerative Laboratory, China) were cultured in Essential 8 (E8) medium (Stem cell, Canada) in 6-well plates with pre-coated Matrigel (Corning, USA). For passaging, the cells were gently washed with phosphate buffer saline (PBS) (Thermo Fisher Scientific, USA), incubated with cell dissociation solution (PBS containing 1.8 g/L NaCl and 0.5 mM EDTA (Solarbio, China), followed by pipetting with appropriate amount of E8 medium. The Y-27632 (10 μM; Stem cell) was added in the culture medium after each splitting.

Construction of lentiviral plasmid and package. The *FTH1* fragment was synthesized according to the Genebank sequence NM_012848 (by GENEWIZ Biotechnology company, China) and cloned into the T vector. *FTH1* was further amplified to have a fragment with blunt ends by using the primers as follows: 5'-CGGTGAATTCCTCGAGACTAGTTCTAGAGCCACCATGACCACCGCGTCT-3' and 3'-CTCCTCGCCCTTGCTCACCATGATACCGGTAGGGCCGGGATTCTCCTCCA-5'. The fragment was cloned into the plasmid pLVX-EGFP (MiaoLing Plasmid, China) by seamless cloning to construct the plasmid pLVX-FTH1-T2A-EGFP. The *iRFP* was amplified by PCR from the plasmid TET-O-FUW-T2A-iRFP (kindly provided by Prof. Zhang) by using the primers: 5'-CCTGGGACACGGTGATGAGAGCGGATCCGAGGGCAGAGGAAGTCTTCT-3' and 3'-TGTTAGAAGACTTCCTCTGCCCTCAGCGCTCTCTTCCATCACGC-5'. The *iRFP* fragment was cloned into the plasmid pLVX-FTH1-T2A-EGFP by seamless cloning method to get a final construct pLVX-FTH1-iRFP-EGFP.

We used four-plasmids packaging system to package lentivirus. The 293T packing cell line (Cell Bank, Chinese Academy of Sciences, China) were maintained in the Dulbecco's Modified Eagle medium (DMEM) (Thermo Fisher Scientific) with 10% (v/v) Fetal Bovine Serum (FBS) (Thermo Fisher Scientific). When the cell density reached 80%, the pLVX-FTH1-iRFP-EGFP and the three package plamids, i.e., pVSV-G (#12259; Addgene, USA), pMDLg (#12251; Addgene), and pRSV-Rev (#12253; Addgene,) were

Table 2. The comparison of the most used in vivo imaging techniques

Imaging modality	Mechanism	Advantages	Disadvantages	Application
MRI	Emitted signal after nuclear spin excitation	(1) High penetration depth (>500 mm) (2) Very good soft tissue contrast (3) High spatial resolution (<100 μm)	(1) Low sensitivity (μM–mM) (2) Provide information at anatomical level	Imaging at anatomical level
PET/SPECT[a]	Photon emission	(1) High sensitivity (nM) (2) Provide quantitative and tomographic information (3) High penetration depth (>500 mm)	(1) Poor spatial resolution (0.5–2 mm) (2) Use of radioactive agents	Imaging at molecular level
Optical imaging	Fluorescence or bioluminescence light emission	(1) High sensitivity (nM) (2) Low cost and high throughput	(1) Limited tissue penetration depth (1–10 mm) (2) Low spatial resolution (1 mm)	Imaging at molecular level
Photoacoustic imaging	Acoustic responses in tissue	(1) High spatial resolution (2) Low cost	limited deep tissue penetration (5 cm)	Imaging at anatomical level

[a] Single photon emission computed tomography (SPECT) and positron emission tomography (PET).

co-transfected the cells by using Lipofectamine 2000 (Thermo Fisher Scientific). VSV-G was the envelope protein for the recombinant vector pseudotyping. The medium containing virus was collected 48 h after transfection, followed by centrifugation at 1000 *g* for 10 min at 4°C. The supernatant was collected, and concentrated by using Lenti-x concentration kit (TaKaRa, Japan). The pellets were re-suspended with appropriate amount of PBS (1/10–1/100 of the original volume) and stored at –80°C for further experiments.

Infection of iPSCs with lentivirus. The lentivirus FTH1-iRFP-EGFP (V_{fre}) was added at a dose of Multiplicity of Infection (MOI) value 2 to 5 together with 2.5 mg/L Polybrene to the iPSC culture for 12 h. Later, the medium containing virus was removed, and fresh E8 medium was added as usual. V_{fre}-infected iPSCs were harvested 48 h after the infection for the subsequent experiments.

Western blot (WB). The sampling of untreated iPSCs, EGFP-infected iPSCs and V_{fre}-infected iPSCs for WB analysis was performed as described before (n = 4 per a group) [10]. Samples were lysed and immunoblotted to detect FTH1 (1 : 1000; Abcam, UK) and β-Actin (1 : 1000; Santa Cruz, USA). The bands were visualized, scanned and quantified with ImageJ (National Institutes of Health, NIH, USA) after subtraction of local background.

In vitro iron uptake assay. EGFP-infected iPSCs or V_{fre}-infected iPSCs were treated with ferric ammonium citrate (FAC; Sigma-Aldrich, USA) in E8 medium at doses of 0, 200 or 500 μM, respectively. After 5 days of culture, the iPSCs was washed by PBS three times to remove free iron ions. Then 10^6 of iPSCs were collected into a 1.5-mL centrifuge tube and fixed by 10 g/L agarose for 15–20 min. The cells were scanned with MRI (MAGNETOM Skyra; SIEMENS, Germany) using the following parameters: Gradient echo, flip angle 20°, repetition time (TR)/echo time (TE) = 3000/82 ms, field of view (FOV) = 60 × 60 mm^2, matrix size = 160 × 120, slice thickness = 2 mm. The images were analyzed with RadiAnt DICOM Viewer software (Medixant, Poland).

V_{fre}-infected iPSCs transplantation into the rat brain. All animal experiments were performed according to the Regulations in China (Regulations for the Administration of Affairs Concerning Experimental Animals, 2017; and approved by the Institutional Animal Care and Use Committee at Chinese Academy of Sciences. Twenty four male SD rats (SPF Biotechnology Co., Ltd. Beijing, China) were subjected to the transplantation surgery and randomly assigned to the subsequent imaging assays. V_{fre}-infected iPSCs were

dissociated and re-suspended in saline at a density of 10^6 cells/μL. 6×10^6 of V_{fre}-infected iPSCs in 6 μL of saline were injected into the left striatum of rats at two of the following coordinates (AP: +1.2 mm; ML: +2.2 mm; DV: −4.0 and −6.0 mm). The same amount of saline was injected into the right striatum at the corresponding coordinates as a self-control for each rat. Transplantation was performed at a rate of 1 μL/min for 3 min, leaving the needle in place for 5 min and slowly lifting it out. After the surgical procedure, animals were monitored for recovery and returned to the home cage.

In vivo MRI. For in vivo MRI, the rats transplanted with V_{fre}-infected iPSCs were anesthetized with 10% chloral hydrate, and scanned 3rd, 9th, 15th, 21th, 27th and 60th day after the surgery. MRI was conducted at a 3.0 T MRI scanner using a 2-cm dual surface coil. T2-weighted signal was acquired using the following parameters to image: Gradient echo, flip angle 20°, TR/TE = 3000/82 ms, FOV = 60×60 mm^2, matrix size = 160×120, slice thickness = 2 mm. The data were analyzed with RadiAnt DICOM Viewer software.

Near-infrared fluorescence (NIF) imaging. The NIF imaging was performed by using the Kodak In-Vivo MultiSpectral Imaging System FX (Kodak, USA) on the rats 3, 9 and 15 days after the transplantation surgery. Rats were anesthetized in a holding chamber of the anesthetic gas machine (RWD Life Science, China) with 40 g/L isoflurane (RWD Life Science). The anesthetized animals were placed in the imaging system and scanned using NIF at a setting of 663/682 nm (excitation/emission), 60 s exposure and 3.0 cm camera height. A sustained ventilation with 2.0–3.5% (v/v) isoflurane was provided during the scanning process to keep the rats still.

Immunohistochemistry and Prussian blue stain. Rats were perfused with 4% paraformaldehyde 30 days or 60 days after the transplantation surgery. The brains were carefully removed, dehydrated with sucrose and flash-frozen in dry ice/isopentane and subsequently stored at −80°C until sectioning. Serial coronal cryosection at a thickness of 30 μm over the striatum were prepared. The sections were blocked with 30 g/L BSA in PBST, sequentially incubated with antisera against GFP (1 : 1000; Abcam). Immunoreactivity was visualized using appropriate Alexa Fluor-conjugated secondary antibodies (Invitrogen, USA). DAPI (Beyotime, China) was counterstained for 15 min. Images were acquired with Laser scanning confocal microscope (Zeiss, Germany).

The cryosections of rat brain were evaluated for iron deposits by using Prussian Blue Staining Kit (Solarbio, China). The working solution was prepared by mixing equal volume of 200 g/L hydrochloric acid and 100 g/L potassium ferrocyanide just before use. The sections were incubated with the working solution, washed and counterstained with nuclear fast red.

RESULTS

Preparation and Identification of the Lentivirus Carrying Multiple Reporter Genes

The lentiviral plasmid carrying multiple reporters was constructed by inserting the reporter *FTH1* gene and *iRFP* fragments into the pLVX-EGFP expressing plasmid. To avoid the conformational interaction of the adjacent reporter proteins, a T2A linker was inserted between two genes (Fig. 1a). To verify if the *FTH1* and *iRFP* fragments were successfully inserted, pLVX-FTH1-iRFP-EGFP was digested by XbaI/BamHI and BamHI/AfeI endonucleases, the *FTH1* (546 bp) and *iRFP* (948 bp) fragments with proper size were observed by electrophoresis (Figs. 1b, 1c).

We next tested if the virus carrying multiple reporters could be produced. By introducing the lentiviral plasmid pLVX-FTH1-iRFP-EGFP and helper plasmids into the 293T packaging cell line, we observed clear fluorescence from EGFP and iRFP exogenous proteins in 293T cells (Fig. 1d).

Stable Expression of FTH1, iRFP and EGFP Reporters in iPSCs

iPSCs could be obtained from the patient's somatic cells and processed multi-differentiation capacity, thus having great potential in the clinics [11]. To evaluate if lentivirus carrying *FTH1*, *iRFP* and *egfp* genes (V_{fre}) properly infected iPSCs, V_{fre} was introduced to the iPSCs culture and fluorescence of EGFP and iRFP was checked 48 h after the infection. Both the green fluorescence from EGFP and the red fluorescence from iRFP could be clearly observed in the iPSCs (Fig. 2a), indicating the integration of these two exogenous genes. A further flow cytometric analysis of EGFP fluorescence showed the EGFP expression in about 34% of the iPSCs treated with V_{fre} (Fig. 2b).

The expression of FTH1 in iPSCs was evaluated by WB. iPSCs were infected with either EGFP-lentivirus or V_{fre}, and lysed for WB analysis 48 h after the infection. As shown in Fig. 2c, there was FTH1 band in the sample from iPSCs infected with V_{fre}, but not in the one from iPSCs infected with EGFP. To evaluate if the iPSCs expressing FTH1 could absorb iron for MRI imaging, we treated the V_{fre}-infected iPSCs with FAC at different dose. As expected, V_{fre}-infected iPSCs showed a dose-dependent increase of iron signal in MRI imaging (Fig. 2d), indicating that exogenous FTH1 in iPSCs has the function of iron uptake.

Long-term in vivo Imaging of V_{fre}-infected iPSCs in the Brain

Cell therapy is a promising strategy for many neurodegenerative diseases such as Parkinson's disease [12]. Meanwhile, the living imaging in the central nervous system remains difficult because of the existence

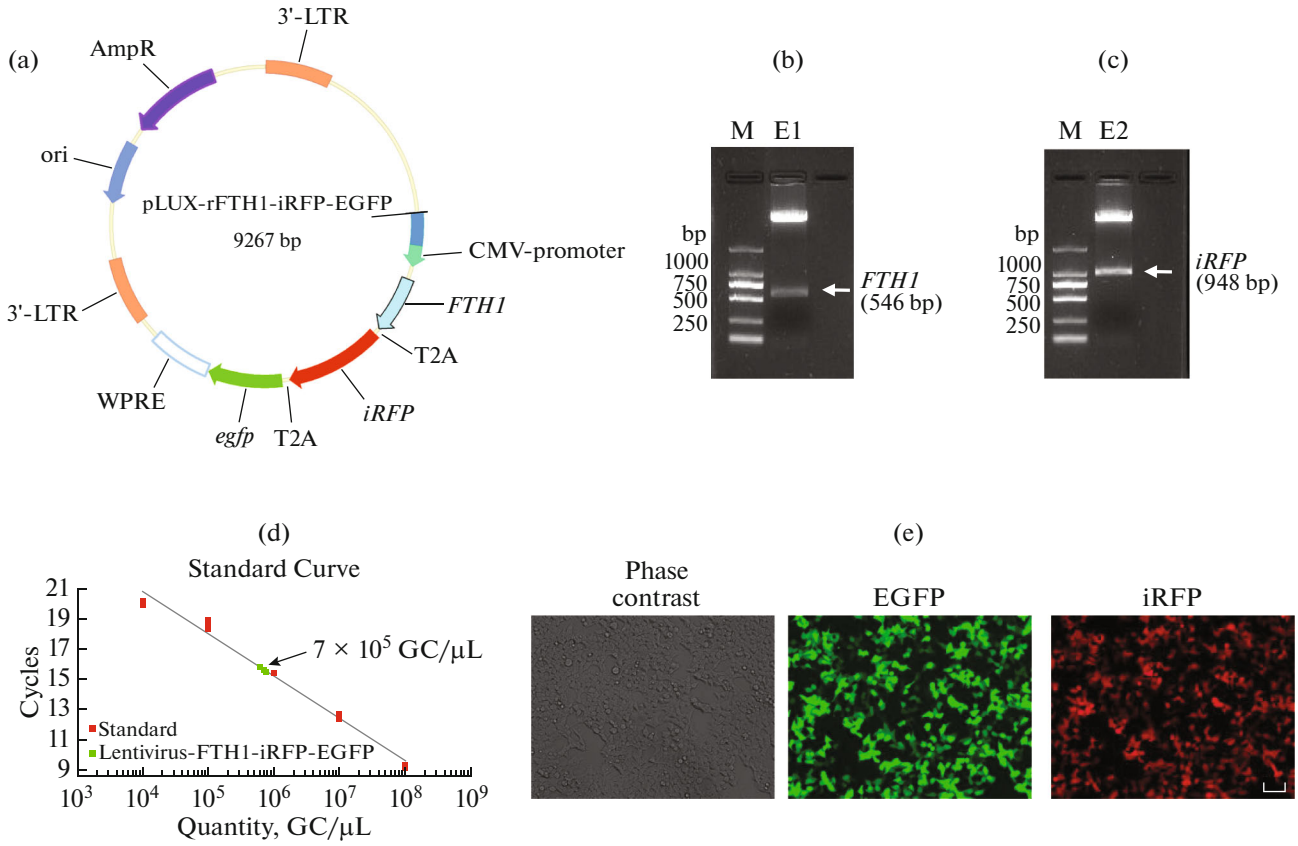

Fig. 1. The preparation of lentivirus carrying *FTH1*, *iRFP* and *egfp* reporter genes. (a) The map of lentiviral plasmid pLVX-FTH1-iRFP-EGFP. WPRE is posttranscriptional regulatory element. (b) The lentiviral plasmid pLVX-FTH1-iRFP-EGFP was digested with XbaI and BamHI, followed by electrophoresis in the lane marked with E1. An expected *FTH1* fragment with the size of 546 bp was indicated by white arrows. (c) The lentiviral plasmid pLVX-FTH1-iRFP-EGFP was digested with BamHI and AfeI, followed by electrophoresis in the lane marked with E2. An expected *iRFP* fragment with the size of 948 bp was indicated by white arrows. The lane marked with M was loaded with DNA marker 2000. (d) The standard curve for titer evaluation of lentivirus carrying *FTH1*, *iRFP* and *egfp*. (e) The green fluorescence of EGFP and NIF of iRFP could be observed in 293T packing cell line transfected with pLVX-FTH1-iRFP-EGFP lentiviral plasmid. Scale bar: 20 μm.

of skull. Therefore, we next tested if the iPSCs carrying multiple reporter genes could be long-term traced in the brain of the living animals. By transplanting the V_{fre}-infected iPSCs into the striatum of rat brain, we performed MRI and NIF imaging 3, 9, 15, 21, 27 and 60 days after the transplantation. iPSCs were administrated unilaterally, and saline was injected contralaterally as a self-control (Fig. 3a). As shown in Fig. 3b, NIF of iRFP could be observed on the 3rd day after transplantation, however, the iRFP signal diminish rapidly, becoming obscure on the 9th day and invisible on the 15th day (Fig. 3b). In contrast, the iron signal from FTH1 checked by MRI was weak on the 3rd day, and the intensity increased with time; a clear MRI signal from V_{fre}-infected iPSCs could be observed from the 9th day till the 60th day after transplantation (Fig. 3c). Neither near-infrared fluorescence nor iron signal from the control side could be observed (Fig. 3b and 3c). All of these results indicated that the V_{fre}-infected iPSCs has the potential to be long-term traced in the brain by in vivo imaging.

Histological Tracing of the V_{fre}-infected iPSCs in the Brain

We next checked, if V_{fre}-infected iPSCs could be observed at the cellular level by histological method, after tracing these cells anatomically by MRI and NIF imaging. The rat brain were perfused 30 or 60 days after the transplantation surgery, sectioned and subjected to either EGFP immunostaining or Prussian blue stain. EGFP-immunopositive cells were observed at the transplanting site both 30 and 60 days after the surgery (Fig. 4a), suggesting that these transplanted iPSCs could survive in vivo for at least 2 months. We also found clear iron deposits around the transplanting sites on the 30th and 60th day by using Prussian blue stain (Fig. 4b), having confirmed the validity of the data on MRI imaging. These observations, together with the results of in vivo imaging, indicated that the engrafted iPSCs carrying FTH1, iRFP and EGFP reporters could be long-term traced in the brain, both at the macroscopic and microscopic level.

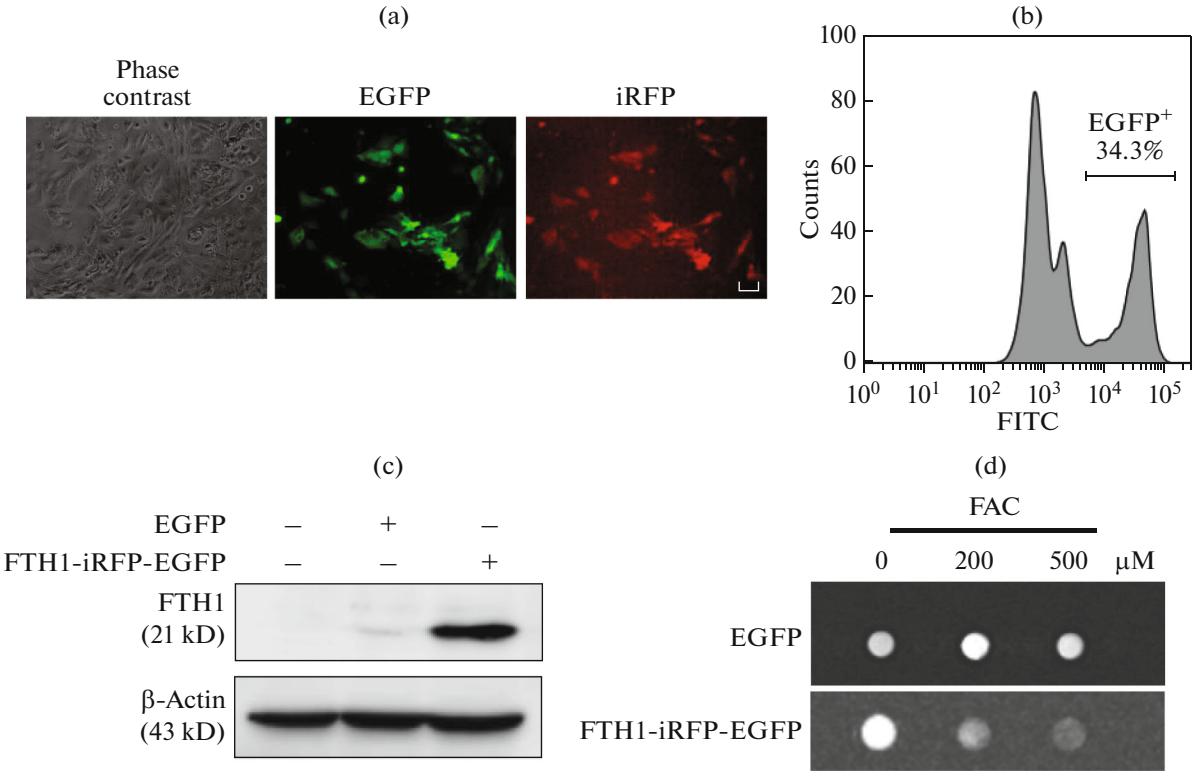

Fig. 2. The stable expression of FTH1, iRFP and EGFP reporters in iPSCs. The iPSCs culture was infected with V_{fre}, and examined for fluorescence 48 h after infection. (a) The representative image of V_{fre}-infected iPSCs under the white light irradiation as well as under the laser excited at 488 nm and 650 nm for EGFP and iRFP detection. (b) The flow cytometric analysis revealed the EGFP expression in about 34% of the iPSCs treated with V_{fre} ($EGFP^+$). (c) WB showing that FTH1 protein is only in the iPSCs infected with V_{fre}. There is FTH1 band neither in the untreated iPSCs nor EGFP-infected iPSC samples subjected for WB. (d) The representative imaging of MRI showing the iron uptake of V_{fre}-infected iPSCs treated with FAC at a concentration of 0, 200 or 500 μM. Note a dose-dependent increase of T2-weighted signal in V_{fre}-infected iPSCs with increasing iron concentration, and no signal in the EGFP-infected iPSCs. Scale bar: 20 μm.

DISCUSSION

The ideal imaging method for cell therapy should have the properties of high imaging specificity and sensitivity, with minimal toxicity [13]. Labeling the target cells with lentivirus carrying reporter genes is probably one of the most ideal tools at present [4]. By using a lentiviral vector, the exogenous reporters could be integrated into cell genome and transmitted to the daughter cells, thus providing very specific and stable cell tracking in vivo with little toxicity [14]. A combination of multiple reporter genes in one lentiviral vector could further avoid the limitations of a single imaging method and increase the sensitivity at different levels. In the present study, we integrated *FTH1*, *iRFP* and *egfp* reporter genes in the one lentiviral vector, which made a long-term and specific imaging of the transplanted iPSCs in the brain at both anatomical and molecular levels feasible.

Among the three reporter genes, *FTH1* encodes the heavy subunit of ferritin, which plays a role in the delivery of iron to cells and storage of iron in a soluble and non-toxic state [15]. The paramagnetism of iron-accumulating cells reduces the T2-weighted relaxation time, thus showing lower T2-weighted signal than the surrounding tissues in MRI imaging [16]. EGFP labeling is very specific and non-toxic, having been widely used to for cell tracking [17]. However, due to its limited penetration depth, it was hardly detected by in vivo fluorescent imaging [17]. iRFP proteins have absorption and emission peaks in the near infrared region, thus having a much better imaging depth and clarity than fluorescent proteins in the visible spectrum [18]. A combination of these three genes could therefore realize a simultaneous detection of MRI signal and optical signals from the transplanted iPSCs.

We observed that the signals of MRI and the NIF from the transplanted cells was not completely overlapped. NIF signal was very clear 3 days after the transplantation, becoming faint on the 9th day and invisible on the 15th day. In contrast, MRI signal is not detectable on the 3rd day, starting to be visible on the 9th day and lasting for 60 days. The attenuation of NIF signal indicated that large number of the transplanted

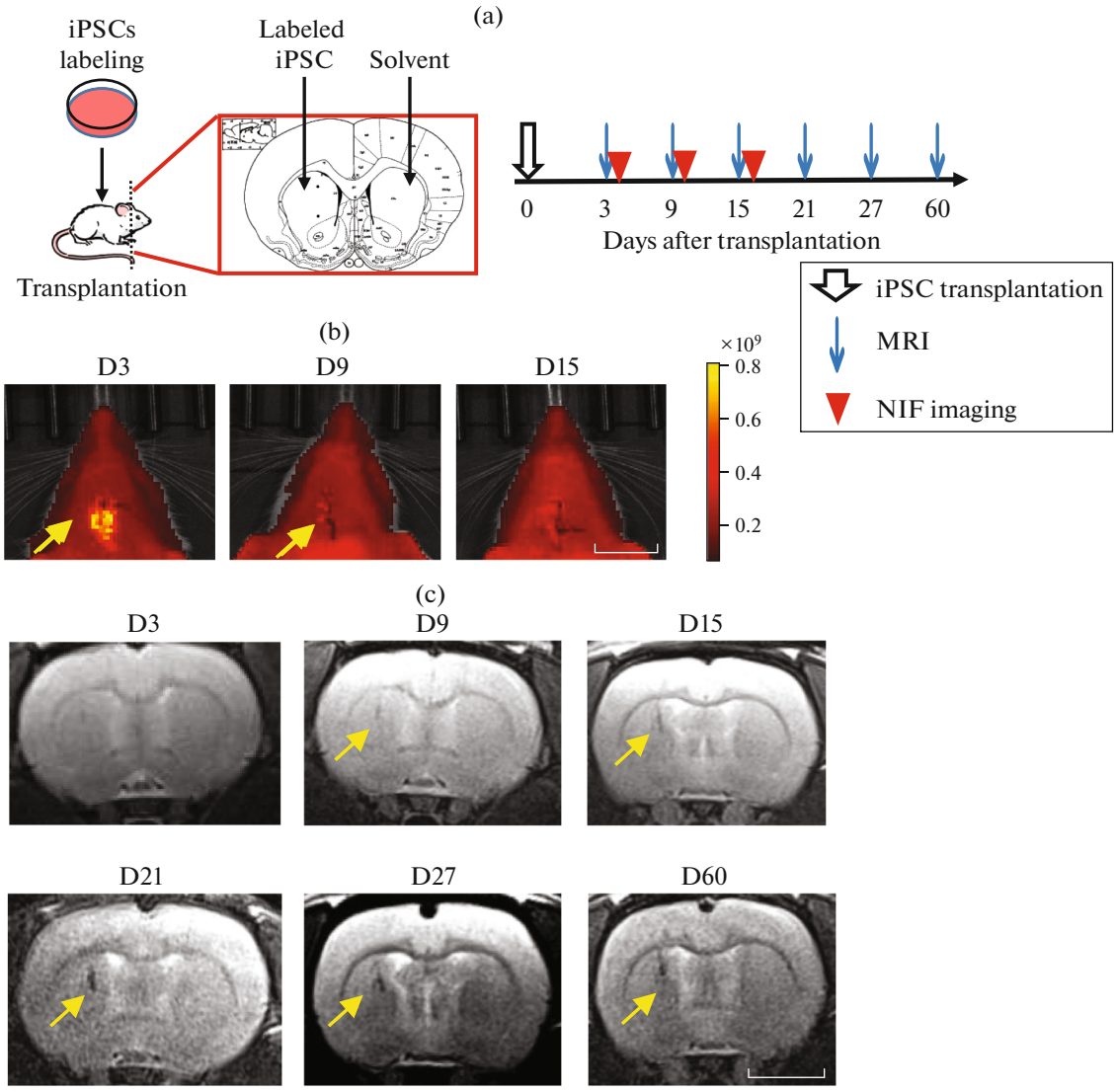

Fig. 3. In vivo MRI and NIF imaging of the rat brain transplanted with V_{fre}-infected iPSCs. (a) The schematic paradigm of the in vivo imaging experiment. The V_{fre}-infected iPSCs (about 6×10^6 cells) in 6 μL of saline were transplanted into the left side of rat striatum, and another 6 μL of saline was injected contralaterally to serve as self-control. (b) NIF images showing the in vivo iRFP fluorescence in the brain transplanted with V_{fre}-infected iPSCs on the 3rd, 9th and 15th day (D3, D9 and D15, respectively) after the surgery. Arrows indicated the iRFP fluorescence from V_{fre}-infected iPSCs at the transplanting site. (c) MRI images showing the T2-weighted signal in the brain transplanted with V_{fre}-infected iPSCs on the 3rd, 9th, 15th, 21th, 27th and 60th day (D3, D9, D15, D21, D27 and D60, respectively) after the surgery. Note, the T2-weighted signal at the transplanting site became visible on the 9th day and persisted until the 60th day after the transplantation. Arrows indicated the T2-weighted signal from V_{fre}-infected iPSCs at the transplanting site. No such signal could be observed in the right side of the brain, which was injected with saline. Scale bar: 5 mm.

iPSCs died shortly after the transplantation surgery, which might because of the injury of surgery and maladaptation to a new niche. Differently, there is a delay of MRI signal since it needs time for FTH1 to accumulate detectable iron from the surrounding tissue. Considering that NIF signal was blocked by skull and brain tissue (the imaging depth is 4.0 cm to 6.0 cm from the skull), it is reasonable to have the observation that the sensitivity of MRI is superior to that of NIF imaging for tracing cells in the deep brain. These data also suggest that a multimodal imaging model could avoid the limitations of different imaging methods and realize a better trace.

Indeed, various multimodal imaging methods have been developed in the recent years and have exhibited overwhelming superiority to a single imaging method

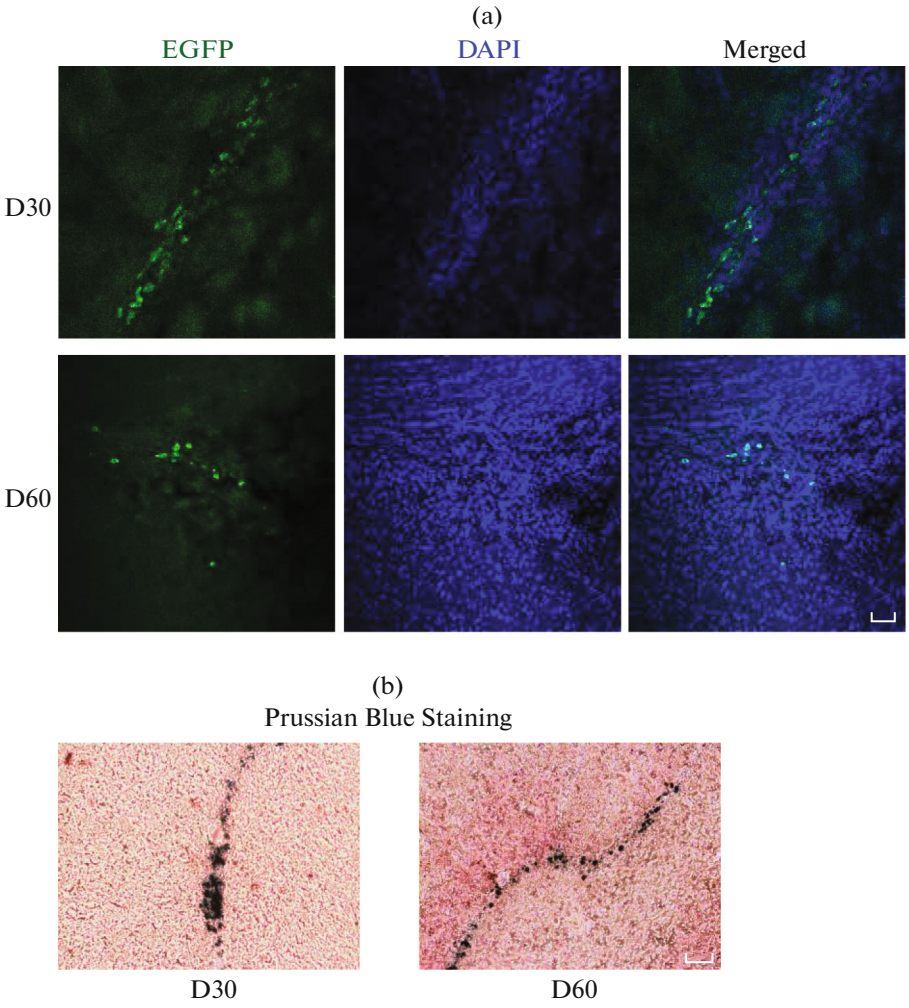

Fig. 4. Imaging of the rat brain transplanted with V_{fre}-infected iPSCs at the cellular level. (a) Representative microscopic image of the striatum in the rats transplanted with V_{fre}-infected iPSCs for 30 days (D30) and 60 days (D60). Sections were stained with anti-EGFP antibody and counterstained with DAPI. (b) Sections from the striatum of rats transplanted with V_{fre}-infected iPSCs for 30 days (D30) and 60 days (D60) were stained for Prussian blue staining. Iron deposits could be observed both on 30th and 60th day after the transplantation. Scale bar: 50 μm in (a); 20 μm in (b).

[4, 19–21]. For example, the targeted radionuclide and fluorescence dual-modality significantly enhance the positioning of the tumor border and effectively guide the surgical resection of the tumor [19]. Kim et al. [20] developed a bimodal lentiviral vector to monitor deep tissue events using MRI by FTH and BFI by GFP, and showed that the MRI and optical imaging can provide an extra level of quantitative and high-resolution information. In the stem cell transplantation therapy, De Vocht et al. [21] established a combined labeling strategy and proved that labeling of Luciferase/EGFP-expressing bone marrow-derived stromal cells with fluorescent micron-sized iron oxide particles improves quantitative and qualitative multimodal imaging of cellular grafts. Similarly, our study has established a multimodal imaging system, which realized simultaneous detection of MRI signal and optical signals including green and NIF, thus providing a new alternative for the cell tracking strategies in the study of cell therapy.

ACKNOWLEDGMENTS

We thank all the laboratory members for their valuable suggestion and kind help.

FUNDING

This study was funded by the Key Research and Development Program of Jiangsu Province, China (Grant

nos. BE2017669 and BE2018668), the National Nature Science Foundation of China (Grant no. 81701332 to S. Yu), the Key Areas Research and Development Program of Guangdong (2019B020235001), the Major Innovative Research Team of Suzhou, China (Grant no. ZXT2019007), and the Natural Science Foundation of Tianjin (Grant no. 17JCYBJC43400).

COMPLIANCE WITH ETHICAL STANDARDS

Conflict of interest. All authors declare no conflict of interest.

Statement on the welfare of animals. All animal experiments were performed according to the Regulations in China (Regulations for the Administration of Affairs Concerning Experimental Animals, 2017) and approved by the Institutional Animal Care and Use committee at Chinese Academy of Sciences. This article does not contain any studies with human participants.

OPEN ACCESS

ADDITIONAL INFORMATION

The text was submitted by the author(s) in English.

REFERENCES

1. Balistreri C.R., Falco E.D., Bordin A., Maslova O., Koliada A., Vaiserman A. 2020. Stem cell therapy: Old challenges and new solutions. *Mol. Biol. Rep*. **47**, 3117–3131.
2. Singh S.P., Rahman M.F., Murty U.S., Mahboob M., Grover P. 2013. Comparative study of genotoxicity and tissue distribution of nano and micron sized iron oxide in rats after acute oral treatment. *Toxicol. Appl. Pharmacol*. **266**, 56–66.
3. Naumova A.V., Balu N., Yarnykh V.L., Reinecke H., Murry C.E., Yuan C. 2014. Magnetic resonance imaging tracking of graft survival in the infarcted heart: iron oxide particles versus ferritin overexpression approach. *J. Cardiovasc. Pharmacol. Ther*. **19**, 358–367.
4. Li M., Wang Y., Liu M., Lan X. 2018. Multimodality reporter gene imaging: construction strategies and application. *Theranostics*. **8**, 2954–2973.
5. Lippincott-Schwartz J., Patterson G.H. 2003. Development and use of fluorescent protein markers in living cells. *Science*. **300**, 87–91.
6. Gu E., Chen W.Y., Gu J., Burridge P., Wu J.C. 2012. Molecular imaging of stem cells: tracking survival, biodistribution, tumorigenicity, and immunogenicity. *Theranostics*. **2**, 335–345.
7. Walter A., Paul-Gilloteaux P., Plochberger B., Plochberger B., Sefc L., Verkade P., Mannheim J.G., Slezak P., Unterhuber A., Marchetti-Deschmann M., Ogris M., Bühler K., Fixler D., Geyer S.H., Weninger W.J., et al. 2020. Correlated multimodal imaging in life sciences: expanding the biomedical horizon. *Front. Phys*. **8**, 47.
8. Zhang W., Zhang S., Xu W., Zhang M., Zhou Q., Chen W. 2017. The function and magnetic resonance imaging of immature dendritic cells under ultrasmall superparamagnetic iron oxide (USPIO)-labeling. *Biotechnol. Lett*. **39**, 1079–1089.
9. Ngen E.J., Artemov D. 2017. Advances in monitoring cell-based therapies with magnetic resonance imaging: future perspectives. *J. Int. Mol. Sci*. **18**, 198.
10. Chen Q., Wang F., Zhang Y., Liu Y., An L., Ma Z., Zhang J., Yu S. 2020. Neonatal DEX exposure leads to hyperanxious and depressive-like behaviors as well as a persistent reduction of BDNF expression in developmental stages. *Biochem. Biophys. Res. Commun*. **527**, 311–316.
11. Hockemeyer D., Jaenisch R. 2016. Induced pluripotent stem cells meet genome editing. *Cell Stem Cell*. **18**, 573–586.
12. Ahmadian-Moghadam H., Sadat-Shirazi M.S., Zarrindast M.R. 2020. Therapeutic potential of stem cells for treatment of neurodegenerative diseases. *Biotechnol. Lett*. **42**, 1073–1101.
13. Nguyen P.K., Lan F., Wang Y., Wu J.C. 2011. Imaging: Guiding the clinical translation of cardiac stem cell therapy. *Circ. Res*. **109**, 962–979.
14. Palfi S., Gurruchaga J.M., Lepetit H., Howard K., Ralph G.S., Mason S., Gouello G., Domenech P., Buttery P.C., Hantraye P., Tuckwell N.J., Barker R.A., Mitrophanous K.A. 2018. Long-term follow-up of a phase I/II study of ProSavin, a lentiviral vector gene therapy for Parkinson's disease. *Hum. Gene Ther. Clin. Dev*. **29**, 148–155.
15. Chiou B., Neely E.B., Mcdevitt D.S., Simpson I.A., Connor J.R. 2020. Transferrin and H-ferritin involvement in brain iron acquisition during postnatal development: impact of sex and genotype. *J. Neurochem*. **152**, 381–396.
16. Dai H., He R., Zhang Y., Wu R.H., Xiao Y.Y. 2017. Adenoviral vector mediated ferritin over-expression in mesenchymal stem cells detected by 7T MRI *in vitro*. *PloS One*. **12**, e0185260.
17. Ansari A.M., Ahmed A.K., Matsangos A.E., Lay F., Born L.J., Marti G., Harmon J.W., Sun Z. 2016. Cellular GFP toxicity and immunogenicity: Potential con-

founders in in vivo cell tracking experiments. *Stem. Cell. Rev. Rep*. **12**, 553–559.

18. Rogers O.C., Johnson D.M., Firnberg E. 2019. mRhubarb: Engineering of monomeric, red-shifted, and brighter variants of iRFP using structure-guided multisite mutagenesis. *Sci. Rep*. **9**, 15653.

19. Lütje S., Rijpkema M., Helfrich W., Oyen W.J., Boerman O.C. 2014. Targeted radionuclide and fluorescence dual-modality imaging of cancer: preclinical advances and clinical translation. *Mol. Imaging. Biol*. **16**, 747–755.

20. Kim H.S., Cho H.R., Choi S.H., Woo J.S., Moon W.K. 2010. In vivo imaging of tumor transduced with bimodal lentiviral vector encoding human ferritin and green fluorescent protein on a 1.5T clinical magnetic resonance scanner. *Cancer. Res*. **70**, 7315–7324.

21. Vocht N.D., Bergwerf I., Vanhoutte G., Daans J., Visscher G.D., Chatterjee S., Pauwels P., Berneman Z., Ponsaerts P., Van der Linden A. 2011. Labeling of luciferase/eGFP-expressing bone marrow-derived stromal cells with fluorescent micron-sized iron oxide particles improves quantitative and qualitative multimodal imaging of cellular grafts in vivo. *Mol. Imaging. Biol*. **13**, 1133–1145.